Helicity, Taylor Relaxation, Spheromaks: Self-Organizing Plasma

Christopher Raastad

Math 336 Term Paper

June 3 2009

Contents

1 Abstract

Plasma is the fourth state of matter, a fluid of ions and electrons violently striped by high thermal energy governed by Magnetic and Electric forces. A simple fluid model of plasma, magnetohydrodynamics treats plasma as a contiguous fluid governed by a combination of Maxwell's equations and the Navier-Stokes equations. Magnetic Helicity, in simple terms, measures the amount of "linkedness", "knottedness", and "twistedness" of magnetic field lines inside plasma. The discretization and measure of helicity, on its own, is an interesting application of mathematical knot theory. More specifically, helicity is a topologically conserved quantity that in ideal, perfectly conducting, plasma instills rigid topological restrictions allowing no magnetic field line breaks and reconnections. On the other hand, in actual non-ideal plasma with partial ohmic-resistivity, the magnetic field lines are free to break and reconnect subject to topological restrictions of conserved global helicity. Moreover, minimizing total magnetic energy under the constraint of total helicity results in a magnetic field satisfying the force-free equation, $\nabla \times \boldsymbol{B} = \lambda \boldsymbol{B}$ for magnetic field $\boldsymbol{B}$, a process called Taylor Relaxation. This process accounts for the tendency for seemingly stochastically created plasma to evolve over time to a "quiescent" organized state of minimum energy. In a singly connected space with proper initial toroidal and poloidal fields, the resultant is a configuration called a Spheromak with possible applications to fusion energy. Finally in a recent paper, (2000), Rañada, Soler, and Trueba propose a model of the cryptic phenomena Ball lightning (aka. St. Elmos fire) as a "Magnetic Knot" with it's infamous properties governed by helicity invariance and Taylor relaxation [10].

2 Introduction of Key Articles and Overview of the Paper

I formulated a discussion on helicity, Taylor relaxation, spheromaks, and ball lightning from major ideas from a a collection of key papers with details filled in by two well written plasma textbooks. J. B. Taylors two key papers, *Relaxation of Toroidal Plasma and Generation of Reverse Magnetic Fields* (1974) [11] and *Relaxation and magnetic reconnection in plasmas* (1986) [12] are highly referenced works discussing the plasma relaxation process, later named, Taylor relaxation. The first is a short, mostly expository summary of results of minimizing magnetic energy under the constraints of both global and local helicity, hence stating the force free equation $\nabla \times \boldsymbol{B} = \lambda \boldsymbol{B}$, and listing the magnetic field solutions for cylindrical coordinates. Taylor's second paper summarizes applying Taylor Relaxation to a multitude of plasma confinement geometries with well derived solutions of the spheromak configuration, that is, a singly connected (like a sphere) containment geometry. His discussion of helicity itself is somewhat minimal, nonintuitive, and uninteresting. Fortunately, I stumbled over Pfister and Gekelman's paper *Demonstration of helicity conservation during magnetic reconnection using Christmas ribbons* (1998) [7], a quite expository but very intuitive discussion that clearly shows how helicity measures the twistedness, linkedness, and knottedness of magnetic field lines with entertaining activities, demonstrations, and clear visualizations. In addition, the paper acts a springboard to further reading, providing nearly 40 citations, more than half extremely relevant. Now, the formal mathematical rigor I felt unfulfilled by previous discussions of helicity was alleviated by H. K. Moffatt and Renzo L. Ricca's *Helicity and the Calugareanu Invariant* (1992), a rigorous, knot theoretical, treatment of helicity which, under the knot theory Calugareanu invariant, can be quantified from the quantities self-linking number, writhe, and twist of a magnetic flux tubes. In addition, Moffatt and Ricca discuss analytic, differential geometry methods to compute these key terms and helicity. Next, one particular work of Antonio F. Rañada, the mostly expository *Ball lightning as a force-free magnetic knot* (2000) [10], proposes a very enlightening toplogical model for the infamous phenomenon that nicely intertwines helicity and Taylor Relaxation. Finally, I found the discussion of helicity, force-free magnetic fields, and Taylor relaxation in Paul M. Bellan's books *Spheromaks* (2000) [2] and *Fundamentals of Plasma Physics* (2006) [3] to be very helpful in working out the particular details of discussed results.

In a general outline, I introduce the concept of Helicity by proceeding into an intuitive expository discussion of its topological significance. Then I progress through deeper topological meaning, analytical computations, and further definitions of helicity. Then I switch gears, delving more into the derivation of Taylor relaxation and force-free magnetic fields. Next I discuss solutions to the force-free equations, a particular example, the Spheromak configuration. Finally, I finish off by giving an exposition of the keys points of the topological theory of ball lightning.

3 Plasma and Magnetic Fields

3.1 Magnetohydrodynamics

Magnetohydrodynamics (MHD) models plasma as a fluid of charged particles governed by the Maxwell and Navier Stokes equations. I will give a brief definition and description of key equations, taken from [5] with help from Dr. Angus McNabb, essential for the discussion of helicity and Taylor Relaxation.

First, let us define fluid density by $\rho = nm$ where n is the number density, that is the number of particles per unit volume and m is standard mass of the particles and $\boldsymbol{v}$ as fluid velocity. We define the continuity equation as

$$\frac{\partial \rho}{\partial t} + \nabla \cdot (\rho \boldsymbol{v}) = 0.$$

This is similar to the Euler Equation, and is simply the conservation of mass relating change in mass to divergence of the particle velocity field. Now we can rewrite this equation a little more intuitively by distributing the divergence with the product rule,

$$\begin{aligned}\frac{\partial \rho}{\partial t} + \rho \nabla \cdot \boldsymbol{v} + \boldsymbol{v} \cdot \nabla \rho = 0 \\ \frac{d\rho}{dt} + \rho \nabla \cdot \boldsymbol{v} = 0 \\ \frac{d\rho}{dt} = -\rho \nabla \cdot \boldsymbol{v},\end{aligned}$$

which now in the form of total time derivative gives us a measure of flux in particle velocity.

Next we define the pressure evolution equation by

$$\frac{d}{dt}\left(\frac{P}{\rho^{\gamma}}\right) = 0$$

where P is pressure and $\gamma = \frac{5}{3}$. Pressure is usually $P \approx nKT$ where T is temperature, K Boltzmann's constant, and n number of particles. Again, we can write this more intuitively by taking the derivative with product and chain rule

$$\begin{aligned}\frac{d}{dt}[P\rho^{-\gamma}] = P\frac{d}{dt}[\rho^{-\gamma}] + \frac{dP}{dt}\rho^{-\gamma} = -\gamma P \rho^{-\gamma-1}\frac{d\rho}{dt} + \frac{dP}{dt}\rho^{-\gamma} = 0 \\ \frac{dP}{dt}\rho^{-\gamma} = P\rho^{-\gamma}\nabla \cdot \boldsymbol{v} \\ \frac{dP}{dt} = \gamma P \nabla \cdot \boldsymbol{v}\end{aligned}$$

where we substituted the alternate form of the continuity equation in the second step. This new form gives us the total time derivative of pressure in relation to velocity divergence. Note that in this calculation we assumed adiabatic processes, otherwise we would have other diffusion terms.

Next I present Maxwell's equations that define electromagnetism. Let $\boldsymbol{E}$ be the electric field, $\boldsymbol{B}$ be the magnetic field, and $\boldsymbol{J}$ be current. We have Faraday's law

$$\nabla \times \boldsymbol{E} = -\frac{\partial \boldsymbol{B}}{\partial t}$$

describing the relation of $\boldsymbol{E}$ and $\boldsymbol{B}$. Next we have Ohm's law,

$$\boldsymbol{E} + \boldsymbol{v} \times \boldsymbol{B} = k\boldsymbol{J},$$

where k is resistivity, which describes the relation of current and electromagnetic forces. Note that in a perfectly conducting idealization, $k = 0$ Ohm's law becomes $\boldsymbol{E} + \boldsymbol{v} \times \boldsymbol{B} = 0$; we will use this assumption later. Finally we have the global properties of the Magnetic Field, that is

$$\nabla \cdot \boldsymbol{B} = 0$$

meaning there are no magnetic monopoles and that

$$\nabla \times \boldsymbol{B} = \mu_0 \boldsymbol{J}$$

, where μ_0 is the permeability of free space, describing current solely by the magnetic field.

Finally we combine the Navier Stokes and Maxwell equations to get the Force Balance, or momentum evolution, equation

$$\rho \frac{d\boldsymbol{v}}{dt} = \boldsymbol{J} \times \boldsymbol{B} - \nabla P.$$

Note that this is MHD Navier Stokes Equation. The quantity $\boldsymbol{F} \equiv \rho \frac{d\boldsymbol{v}}{dt}$ resembles force, since ρ is a mass distribution and $\frac{dv}{dt}$ vector acceleration. Now we say a system is Force free if the quantity $\rho \frac{dv}{dt} = 0$ meaning $\nabla P = \boldsymbol{J} \times \boldsymbol{B}$.

In addition, we define the useful quantity β cleverly named the Beta of the plasma given by

$$\beta = \frac{P}{\mu_0 B^2}$$

where $B = |\boldsymbol{B}|$. This quantity essentially gives us a ratio of hydrodynamic pressure to magnetic pressure in a plasma. In simple terms, magnetic pressure is the tendency for a plasma configuration to expand and pinch due to magnetic and current forces. Consider a simple analogy, a toroidal shaped plasma will tend to evolve from an initial shape resembling a thick small vespa tire to a thin large bicycle tire. So, in consequence, a plasma with small β will be governed by mostly electromagnetic forces while a plasma with high β will be governed by mostly hydrodynamic fluid forces.

As a final note, if a plasma has very small β we can assume the pressure gradient term in the force balance equations $\nabla p \approx 0$ and is negligible. Moreover, if the plasma is force free and low β, then $\boldsymbol{J} \times \boldsymbol{B} = 0$ is the force balance equation.

3.2 Toroidal and Poloidal magnetic fields

In discussion of Taylor Relaxation and Spheromaks we will generally be considering toroidal magnetic fields confined in a cylindrical container. In cylindrical coordinates we describe this configuration by $\boldsymbol{B}(r, \phi, z) = B_r \hat{\boldsymbol{r}} + B_\phi \hat{\boldsymbol{\phi}} + B_z \hat{\boldsymbol{z}}$. We consider the quantity $B_r \hat{\boldsymbol{r}} + B_z \hat{\boldsymbol{z}}$ to describe the

Poloidal component of the magnetic field and the quantity $B_\phi \hat{\boldsymbol{\phi}}$ to describe the toroidal component of the magnetic field. The toroidal magnetic field will be aligned such that the hole of the torus is punctured by a line in the direction of the $\hat{\boldsymbol{z}}$ axis of the cylinder. In a Spheromak the toroidal components of field wrap around in the direction of the curvature of the cylinder and the poloidal components wrap around the toroidal component through the hole of the torus. This magnetic field configuration is beautifully visualized in Figure 9, the magnetic streamline plot of a Spheromak.

4 Helicity

4.1 Definition

Since Taylor [11][12] gave a rough derivation of the quantity in his two papers, I will consider Mofatt and Ricca's (1992)[6] rigorous topological treatment of helicity intermingled with the somewhat simpler notation taken from the paper of Pfister and Walter (1990)[7]. Consider a solenoidal vector field $\boldsymbol{A}(\boldsymbol{x}) = \nabla \times \boldsymbol{A}(\boldsymbol{x})$ defined on a set $\Omega \in \mathbb{R}^3$ of compact support, where $\boldsymbol{A}$ is the magnetic vector potential defined by $\nabla \times \boldsymbol{A} = \boldsymbol{B}$ for every $\boldsymbol{x} \in \Omega$. We suppose that $\boldsymbol{B} \cdot d\boldsymbol{S} = \boldsymbol{B} \cdot \hat{\boldsymbol{n}} = 0$ on $\partial\Omega$, the boundary of Ω, where $\hat{\boldsymbol{n}}$ is a normalized normal vector at the boundary oriented outward, that is, all magnetic field lines are contained within Ω; this can be achieved with a perfectly conducting wall. Firstly, we define magnetic flux, Φ, which measures to the amount of magnetic field $\boldsymbol{B}$ that penetrates a cross-sectional area S, as the surface integral

$$\Phi = \int_S \boldsymbol{B} \cdot d\boldsymbol{S}.$$

Then we define the pseudo-scalar quantity helicity K of $\boldsymbol{B}$ by

$$K = \int_\Omega \boldsymbol{A} \cdot \boldsymbol{B}\, dV$$

where $dV = d^3\boldsymbol{x}$ is the volume element and the quantity $\boldsymbol{A} \cdot \boldsymbol{B}$ is integrated over the entire volume Ω where $\boldsymbol{B}$ exists. It is important to question whether this definition makes sense, that is, whether it makes sense to define $\boldsymbol{A} \cdot \boldsymbol{B}$ an intensive property, meaning a physical property that does not depend on the system size and amount of material in the system, and K as an extensive property of a system independent of system size and amount of material. We see the definition of K does make sense as it is gauge invariant. Suppose we perturb $\boldsymbol{A}$ by a scalar function f by letting $\boldsymbol{A}' = \boldsymbol{A} + \nabla f$. We find that $\boldsymbol{B} = \nabla \times (\boldsymbol{A} + \nabla f) = \nabla \times \boldsymbol{A} + \nabla \times (\nabla f) = \boldsymbol{B}$ is unchanged and moreover, since $\boldsymbol{B} \cdot \hat{\boldsymbol{n}} = 0$ by assumption, the integral

$$K' = \int_\Omega \boldsymbol{A'} \cdot \boldsymbol{B}\, dV = \int_\Omega \boldsymbol{A} \cdot \boldsymbol{B}\, dV + \int_\Omega \nabla \cdot (f\boldsymbol{B})\, dV = \int_\Omega \boldsymbol{A} \cdot \boldsymbol{B}\, dV + \int_{\partial\Omega} (f\boldsymbol{B}) \cdot \boldsymbol{n}\, dS = \int_\Omega \boldsymbol{A} \cdot \boldsymbol{B}\, dV = K$$

using the divergence theorem [3]. Thus helicity is invariant under Gauge transformations and so makes sense as a extensive property of the system. Clearly the intuitive meaning of this quantity as a measure of twistedness and knottededness of magnetic field lines is unclear, so consider the following calculation.

4.2 Simple Calculation: Two Singly Linked Flux Tubes

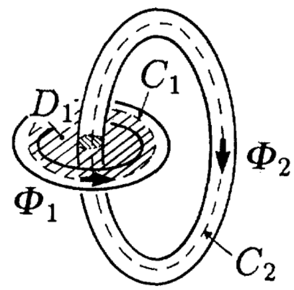

Figure 1: Two linked, oriented, and unknotted flux tubes carrying appropriate uniform flux [6].

A flux tube is simply a region in space with a concentrated uniform magnetic field such that the field on the sides is parallel to the tube. Both cross-sectional area and field containment may very along the length of the tube, but the magnetic flux is always constant. Consider a system where $\boldsymbol{B} = 0$ except in two singly linked magnetic flux tubes C_1 and C_2 with volumes V_1 and V_2 and uniform flux Φ_1 and Φ_2 as in Figure 1. The integral vanish outside V_1 and V_2 so we see the helicity of the configuration is the superposition $K = K_1 + K_2$ where

$$K_1 = \int_{V_1} \boldsymbol{A} \cdot \boldsymbol{B} dV \qquad K_2 = \int_{V_2} \boldsymbol{A} \cdot \boldsymbol{B} dV.$$

Now applying Stokes theorem to our definition of flux above we have

$$\Phi = \int_S \boldsymbol{B} \cdot d\boldsymbol{S} = \int_S (\nabla \times \boldsymbol{A}) \cdot d\boldsymbol{S} = \oint_C \boldsymbol{A} \cdot d\boldsymbol{x}$$

where $d\boldsymbol{S} = \hat{\boldsymbol{n}}\, dS$ denotes a vector normal to the area element dS, $d\boldsymbol{x}$ is the element of length, and C is a closed curve bounding S [7]. So now we can rewrite $dV = d\boldsymbol{S} \cdot d\boldsymbol{x}$ where $\boldsymbol{A} \cdot \boldsymbol{B}\, dV = (\boldsymbol{A} \cdot \boldsymbol{B})(d\boldsymbol{S} \cdot d\boldsymbol{x}) = (\boldsymbol{A} \cdot d\boldsymbol{x})(\boldsymbol{B} \cdot d\boldsymbol{x})$ and so applying Fubini's Theorem to rearrange integral terms we have

$$K_1 = \oint_{C_1} \int_{S_1} (\boldsymbol{A} \cdot d\boldsymbol{x})(\boldsymbol{B} \cdot d\boldsymbol{S}) = \Phi_1 \oint_{C_1} \boldsymbol{A} \cdot d\boldsymbol{x}$$

since $\int_{S_1} \boldsymbol{B} \cdot d\boldsymbol{S} = \Phi_1$ by definition. Now by Stokes theorem we have

$$K_1 = \Phi_1 \oint_{C_1} \boldsymbol{A} \cdot d\boldsymbol{x} = \Phi_1 \int_{D_1} \boldsymbol{B} \cdot \hat{\boldsymbol{n}}\, d\boldsymbol{S} = \Phi_1 \Phi_2$$

since we are only picking up the flux flowing along curve C_2 passing through D_1 which is equal to Φ_2. Thus after calculating K_2 by an identical symmetric argument we have $K = K_1 + K_2 = 2\Phi_1\Phi_2$. [2][6][7]

4.3 Basic Measure of Helicity

We will discuss the three main topological forms of helicity measurement. For simplicity let us discuss a configuration with all flux tubes containing the same flux Φ. We can model measuring helicity contained in a twisted flux tube by drawing a line on the surface of a flux tube and and count how often a given magnetic field line crosses this imaginary line [7].

4.3.1 Writhe

The simplest helicity measurement is a 360° twist in a single flux tube as in Figures 2. This will have helicity contribution of $K = \pm\Phi^2$, which can conceptually be thought of the flux tube 'crossing' itself once [2][7]. The contribution is positive if we twist clockwise moving along the direction of $\boldsymbol{B}$ and negative if we twist counterclockwise moving along the direction of $\boldsymbol{B}$ (which can easily be visualized by using right hand rule with the thumb pointing in the direction of the flux and the fingers curling in a positive direction of the twist). We will define this as our elemental quantum of helicity. Later we will rigorously derive the quantity Φ^2 of a single flux tube from the definition of flux [2, p.43][6, p.417]. Also note that a Mobius strip, a 180° twist will contribute $\pm\frac{1}{2}\Phi^2$, half a unit, of helicity.

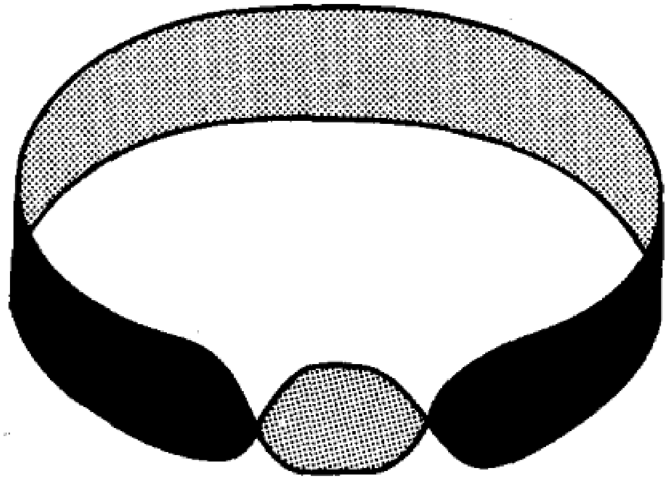

Figure 2: Flux tube with 360° of twist [7].

4.3.2 Crossing

Each crossing, as in Figure 3, of the system contributes $K = \pm\Phi^2$ of helicity [2][7]. Again, the sign can be determined by the right hand rule; pointing your thumb in the direction of the $\boldsymbol{B}$ along one of the flux tubes, if the curl of your fingers coincides with the direction of $\boldsymbol{B}$ along the other flux tube, then K is positive, otherwise K is negative. With a simple experiment we can clearly see how this measurement reduces to the twist case. Take a piece of Christmas Ribbon, like Pfister and Walter, connect the two ends such that we have a nice smooth crossing as Figure 3, then pulling apart the crossing into a circular ribbon to find a 360° twist, as in Figure 2.

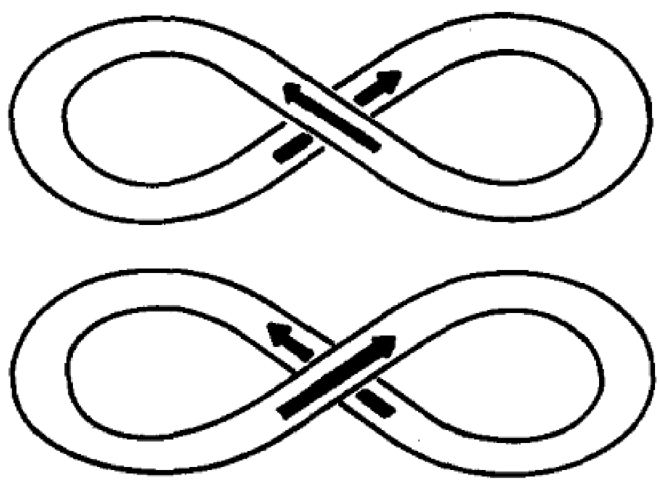

Figure 3: Flux tubes with one crossing and no internal twist. Top tube contributes negative helicity while bottom contributes positive [7].

4.3.3 Linking

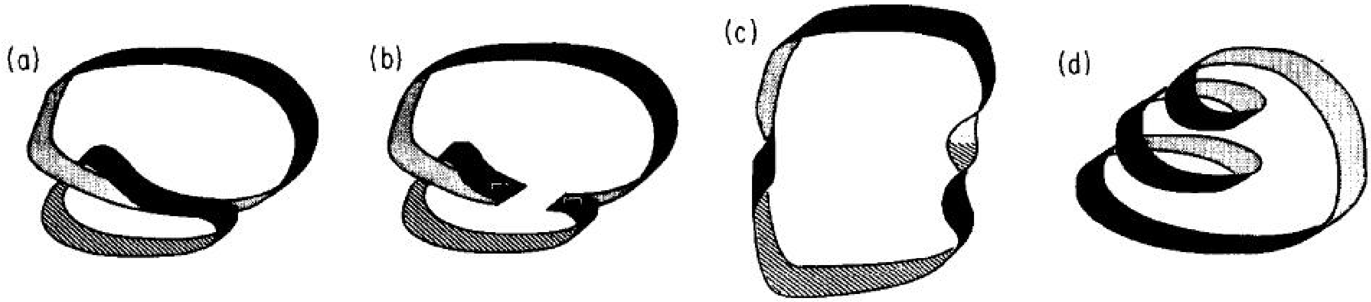

Figure 4: A sequence of helicity conserving operations on two singly linked flux tubes (a). We carefully make a cut in (b) and reconnect and deform in (c) to show two 360° twists and further deform in (d) to show two crosses [7].

Each knot 'link' between two disjoint flux tubes contributes $K = \pm 2\Phi^2$ helicity. Conceptually, each link can be thought of as two singly linked flux tubes, as calculated above in Figure 1 [2][7]. We define K to be positive if the link is a right handed system, that is, point your thumb in one direction of $\boldsymbol{B}$ in one flux tube, if the curl of your fingers points with the direction of $\boldsymbol{B}$ in the other tube, then the system is right handed and contributes $+2K\Phi^2$ positive helicity, otherwise the system is left handed and contributes $-2K\Phi^2$ negative helicity. Also, we can conceptually reduce this case back to twist. Given two singly linked Christmas ribbons, drawing $\boldsymbol{B}$ field arrows on both ribbons, if we cut both ribbons and carefully reconnect them without twisting we will end up with two 360° twists in the ribbon; this is outlined in Figure 4.

4.3.4 More Complex Helicity

For helicity calculations of a more complicated, knotted field line configuration we can use superposition and compute the sum of helicity contributions from the three measurement forms. For a more complicated example, consider the Trefoil Knot, Figure 5. This configuration has 3 crossings, thus a helicity of $K = \pm 3\Phi^2$ (depending on right/left-handedness of the knot, in the Figure 5 we have a right handed knot) [7]. As we will see soon, we can easily apply Mathematical knot theory [1] to any magnetic flux tube knot to compute the helicity.

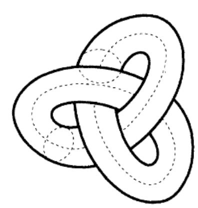

Figure 5: The simplest knot, the trefoil knot.

4.4 Sketch of Derivation of Twist Helicity $K_T = \Phi^2$

Our argument for twist above contained very little mathematical substance. Unfortunately, the rigorous derivation of Twist helicity is unsatisfactorily complicated. Moffatt and Ricca give a brief but uncomprehendingly sophisticated topological/knot theory argument [6]. Bellan's Spheromak book gives a clear but quite lengthy argument employing mostly multivariate calculus techniques with a change to toroidal coordinates carrying very nasty gradient and differential terms. In summary, the analytic argument to compute twisting helicity is based on modeling a writhed toroidal flux tube as a winding toroidal field line with poloidal and toroidal flux (this is easy to visualized in the streamline plot in the Spheromak discussion later). We derive the resulting helicity by taking an infinitesimal approximation combining the two tubes. I will sketch the proof as well paraphrased by Berger and Field's discussion [4].

Consider a volume consisting of nested toroidal magnetic surfaces. Let Ψ_P be the poloidal flux through the whole of the toroidal surface and Ψ_T be the toroidal flux in within the surface. For infintesimal annular volume containing flux, $(d\Psi_T, -d\Psi_P)$, the linkage helicity is with the fields outside counted once is $\Psi_P\, d\Psi_T$. Likewise, the linkage helicity with fields within the surface is $-\Psi_T\, d\Psi_P$. Thus the change in helicity of the annular volume is $dK = \Psi_P\, d\Psi_T - \Psi_T\, d\Psi_P$. Now let $T = -\frac{d\Psi_P}{d\Psi_T}$, represent the number of times a field line winds around the torus in the poloidal ('short way') direction for one circuit in the ('longer') toroidal direction. Then integrating dK from $[0, \Phi]$ where Φ is the total toroidal flux, integrating $\Psi_P\, d\Psi_T$ by parts we have

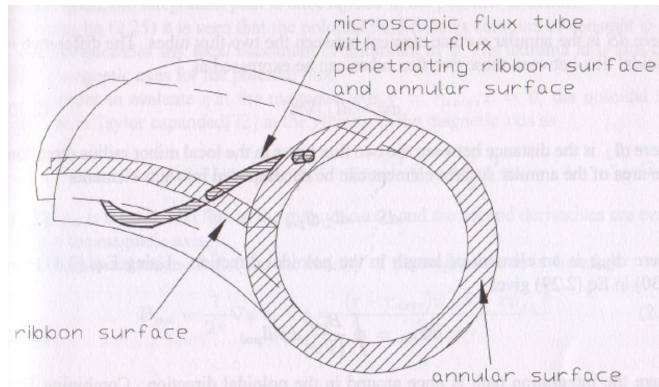

Figure 6: Visual demonstrating toroidal and poloidal components of flux for a helically windy flux tube around a torus [2]

$$\begin{aligned}
\int dH &= \int_0^{\Phi} (\Psi_P\, d\Psi_T - \Psi_T\, d\Psi_P) \\
&= \Psi_P \Psi_T - \int_0^{\Phi} \Psi_T\, d\Psi_P - \int_0^{\Phi} \Psi_T\, d\Psi_P \\
&= \Psi_P \Psi_T + 2 \int_0^{\Phi} T \Psi_T\, d\Psi_T \\
&= T\Phi^2
\end{aligned}$$

for a uniformly twisted torus. Note the $\Psi_P \Psi_T$ term vanishes if we make the assumption that Φ vanishes at the wall of our flux tube and the fact Φ vanishes on the magnetic access (i.e. center of circular slices of tubular part of torus) [2, p.44]. And hence we get the desired results, where $T = 1$, i.e., one 360° twist around the torus.

4.5 Magnetic Reconnection and Helicity Conservation

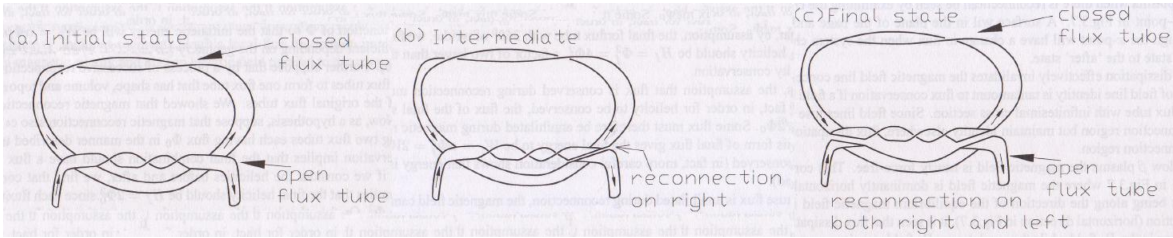

Figure 7: A sequence of helicity conserving magnetic field line breaks and reconnections [2].

In an ideal MHD system, helicity for each flux tube is conserved, that is, the topological knot properties are conserved and there is no breaking or reconnecting of flux tubes. We find, in a non ideal system with small resistivity, local helicity is not conserved. In fact, we find there is magnetic field breaking and reconnection, that is, field lines break and reconnect. Fortunately, as demonstrated by Figure 7, field lines and break and reconnect precisely to conserve global magnetic helicity. [2][11][12]

4.6 The Figure-8 Method

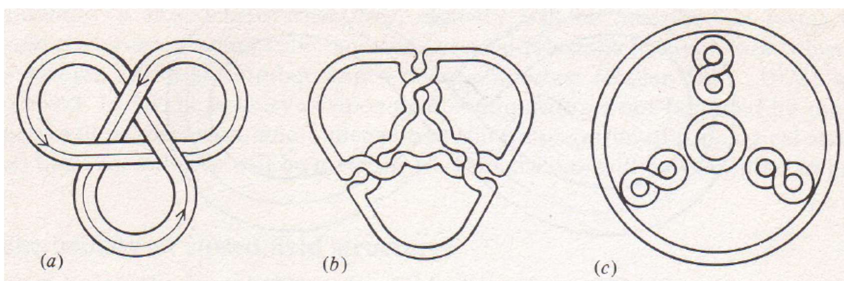

Figure 8: Example of applying helicity conserving breaks and reconnections to derive the helicity of the Trefoil knot [4].

For an arbitrarily twisted, crossed, and knotted flux tube we can express $K = K_T + K_K$ where K_T is the sum of twist helicity and H_K is the sum of knot helicity. Note that this decomposition is not topologically invariant because we can easily convert twists and crosses to one another. We consider an 'untwisted' tube as one in which we can draw a line on top of the tube for its entire length as viewed from a planar projection without the line disappearing under the tube (picture Christmas Ribbon). Now, this line on top of the tube sets $\theta = 0$ in a poloidal coordinate system, and we can measure H_K from the number of crosses.

Alternatively we can measure helicity by applying helicity conserving flux tube disconnections and reconnections as in Figure 8. At each cross over in a flux knot, we helically reconnect each side (making sure field directions align without twists) to create a figure 7. Then we simply sum this figure 8 crossing by their sign either N_+ or N_- defined by the right hand rule on the crossing implying $H_K = \Phi^2(N_+ - N_-)$. With the figure concluding the Trefoil knot has $H = \pm\Phi^2$ depending on orientation.

4.7 Advanced Analytic Measure of Helicity

Now following the reasoning in Moffatt and Rica's paper, we can do more by finding rigorous analytic expressions for the writhing (twisting) and crossing numbers of an arbitrary magnetic flux tube! Suppose a knot K is in the form of a closed curve C containing no inflection points (this can be done for an arbitrary knot by applying continuous deformations). Consider some origin O and define s to be the arc length with respect to this point and suppose there is some parameterization of C given by $\boldsymbol{x} = \boldsymbol{x}(s)$ where $\boldsymbol{x}$ is periodic with respect to L, the length of C. We define the unit tangent vector as $\hat{\boldsymbol{t}} = \frac{d\boldsymbol{x}}{ds}$, the unit principle normal vector $\hat{\boldsymbol{n}} = (\frac{d\hat{\boldsymbol{t}}}{ds})/|\frac{d\hat{\boldsymbol{t}}}{ds}|$, and binomial vector $\hat{\boldsymbol{b}} = \hat{\boldsymbol{t}} \times \hat{\boldsymbol{n}}$ that satisfy the Frenet equations

$$\frac{d\hat{\boldsymbol{t}}}{ds} - \kappa\hat{\boldsymbol{n}}, \qquad \frac{d\hat{\boldsymbol{n}}}{ds} = -\kappa\hat{\boldsymbol{t}} + \tau\hat{\boldsymbol{b}}, \qquad \frac{d\hat{\boldsymbol{b}}}{ds} = -\tau\hat{\boldsymbol{n}},$$

where $\kappa(s)$ is the curvature and $\tau(s)$ is the torsion of C at position s along C. Notice if we had a point of inflection where $\kappa = 0$ then our $\hat{\boldsymbol{n}}, \hat{\boldsymbol{b}}$, and τ would be undefined.

Now let T denote the surface of a flux tube running parallel along C constructed around K with uniform flux Φ. We wish to find the helicity of T by considering the limiting behavior as the cross section of T tends to zero. Now let the magnetic field $\boldsymbol{B} = \boldsymbol{B}_t + \boldsymbol{B}_p$ where $\boldsymbol{B}_t$ is toroidal field in parallel in the direction of tube axis and $\boldsymbol{B}_p$ is poloidal field perpendicular to the tube axis. When the cross section of the tube T is small we can adopt cylindrical coordinates (r, θ, z) and assume we have $\boldsymbol{B}_t = (0, 0, \boldsymbol{B}_z(r))$ and $\boldsymbol{B}_p = (0, \boldsymbol{B}_\theta(r), 0)$. We must have $\nabla \cdot \boldsymbol{B}_t = 0$ and $\nabla \cdot \boldsymbol{B}_p = 0$ to satisfy boundary definitions, hence we can have separate potentials $\boldsymbol{B}_t = \nabla \times \boldsymbol{A}_t$ and $\boldsymbol{B}_p = \nabla \times \boldsymbol{A}_p$ with both $\nabla \cdot \boldsymbol{A}_t = 0$ and $\nabla \times \boldsymbol{A}_p = 0$. Moreover, force field traces of $\boldsymbol{B}_p$ are unlinked circles thus the helicity integral $\int_T \boldsymbol{A}_p \cdot \boldsymbol{B}_p dV = 0$, and hence the helicity of the total field is given by

$$\begin{aligned} K &= \int_T \boldsymbol{A}_t \cdot \boldsymbol{B}_t \, dV + \int_T \boldsymbol{A}_t \cdot \boldsymbol{B}_t \, dV + \int_t \boldsymbol{A}_p \cdot \boldsymbol{B}_t \, dV \\ &= \int_T \boldsymbol{A}_t \cdot \boldsymbol{B}_t \, dV + 2\int_T \boldsymbol{A}_t \cdot \boldsymbol{B}_p \, dV \end{aligned}$$

using integration by parts and divergence theorem over T. Now let us consider both terms of the integral individually.

First we need a reinterpretation of $\boldsymbol{A}$. Recall the vector potential $\boldsymbol{A}$ is defined by $\boldsymbol{B} = \nabla \times \boldsymbol{A}$. But, if we apply a Coulumb gauge for $\boldsymbol{A}$, that is $\nabla \cdot \boldsymbol{A} = 0$ and require $\boldsymbol{A} = O(|\boldsymbol{x}|^{-3})$, meaning $\boldsymbol{A}|\boldsymbol{x}|^{-3} \to 0$ as $|\boldsymbol{x}| \to \infty$ then using the Biot-Savart law we can rewrite $\boldsymbol{A}(\boldsymbol{x})$ as

$$\boldsymbol{A}(\boldsymbol{x}) = \frac{1}{4\pi}\int_{V^*} \frac{\boldsymbol{B}(\boldsymbol{x}^*) \times (\boldsymbol{x} - \boldsymbol{x}^*)}{|\boldsymbol{x} - \boldsymbol{x}^*|^3} dV^*.$$

Moreover, the helicity integral can now be defined as

$$K = \frac{1}{4\pi}\int_V \int_{V^*} \frac{[\boldsymbol{B}(\boldsymbol{x}^*) \times \boldsymbol{B}(\boldsymbol{x})] \cdot (\boldsymbol{x} - \boldsymbol{x}^*)}{|\boldsymbol{x} - \boldsymbol{x}^*|^3} dV^* dV.$$

Now considering the toroidal/axial component $K_t = \int_T \boldsymbol{A}_t \cdot \boldsymbol{B}_t dV$. In the limiting form as the cross section width of T goes to zero we have the Biot-Savart form of $\boldsymbol{A}$ tending to

$$\boldsymbol{A}(\boldsymbol{x}) = \frac{1}{4\pi}\Phi \oint_C \frac{d\boldsymbol{x}^* \times (\boldsymbol{x} - \boldsymbol{x}^*)}{|\boldsymbol{x} - \boldsymbol{x}^*|^3}.$$

which diverges for $\boldsymbol{x} \in C$, but the toroidal/axial component does not diverge, thus the limiting expression for toroidal/axial helicity tends to

$$K_t = \frac{1}{4\pi}\Phi^2 \oint_C \oint_C \frac{(d\boldsymbol{x}^* \times d\boldsymbol{x}) \cdot (\boldsymbol{x} - \boldsymbol{x}^*)}{|\boldsymbol{x} - \boldsymbol{x}^*|^3} = \Phi^2 \mathcal{W}$$

where $\mathcal{W}$ is the writhing (twisting) number of C otherwise called the writhe of C. Like above, if we project C onto a 2-D plane curve with unit normal $\boldsymbol{\nu}$ we can write $\mathcal{W} = \langle n_+(\boldsymbol{\nu}) - n_-(\boldsymbol{\nu})\rangle$ where $n_+(\boldsymbol{\nu})$ is the number of positive crossings and $n_-(\boldsymbol{\nu})$ is the number of negatives crossings by crossing diagrams discussed earlier. With a similar argument we can define the crossing number $\mathcal{C}$ by

$$\mathcal{C} = \frac{1}{4\pi}\Phi^2 \oint_C \oint_C \frac{|(d\boldsymbol{x}^* \times d\boldsymbol{x}) \cdot (\boldsymbol{x} - \boldsymbol{x}^*)|}{|\boldsymbol{x} - \boldsymbol{x}^*|^3}.$$

Note that the integrals for $\mathcal{W}$ and $\mathcal{C}$ are taken over all arc segements for all pairs of elements $d\boldsymbol{x}, d\boldsymbol{x}^*$. Now from a complicated argument (which I conveniently omit) involving differentiating under the integral argument and complicated coordinate transformations, Moffatt and Ricca define the twisting parameter $\mathcal{T}$ as the total torsion normalized by a factor of $2\pi^{-1}$ by

$$\mathcal{T} = \frac{1}{2\pi} \int_C \tau(s)\, ds$$

which we can expressed in a larger pararemter called twist, denoted Tw, computed in terms of a normalized spanwise vector $\boldsymbol{N}$ on the ribbon relative to $(\hat{\boldsymbol{n}}, \hat{\boldsymbol{b}})$ and it's derivative, $\boldsymbol{N'} \equiv \frac{d\boldsymbol{N}}{ds}$ as

$$Tw = \frac{1}{2\pi} \oint_C (\boldsymbol{N'} \times \boldsymbol{N}) \cdot \hat{\boldsymbol{t}}\, ds = \mathcal{T} + \frac{1}{2\pi}[\Theta]_C$$

in which we define $\mathcal{N} = \frac{1}{2\pi}[\Theta]_C$ and they later show that

$$\frac{dK_p}{dt} = \Phi^2 \frac{d\mathcal{T}}{dt}.$$

It follows that $K_m = \Phi^2(\mathcal{T} + \mathcal{T}_0) = \Phi^2(\mathcal{T} + \mathcal{N})$ where $\mathcal{T}_0 \equiv \mathcal{N}$ is the twist parameter (as above, but not to be confused with twist number which is $Tw = \mathcal{T} + \mathcal{N}$), an integer constant representing the number of rotations of unit spanwise vector $\boldsymbol{N}$ on the ribbon relative to Frenet pair $(\hat{\boldsymbol{n}}, \hat{\boldsymbol{b}})$ in one passing around C.

And so finally, we have the Calugareanu invariant, which state the linking number

$$n = \mathcal{W} + Tw = \mathcal{W} + \mathcal{T} + \mathcal{N}$$

where n represents the number of times a flux tube (or arbitrary knot for that matter) crosses itself and hence the helicity is $K = \Phi^2 n$ for a tube of uniform flux Φ.

5 Taylor Relaxation

Now we will discuss, as in J. B. Taylor's paper [11], how helicity plays a role in Taylor Relaxation, a process in which initially violent, unstable relaxes into a "quiescent" stable Taylor state corresponding to a state of minimum energy. Taylor's paper starts with the equation for perfectly conducting fluid variations in a magnetic field, $\frac{\partial \boldsymbol{B}}{\partial t} - \nabla \times (\boldsymbol{v} \times \boldsymbol{B}) = 0$, where $\boldsymbol{v}$ is the fluid velocity, and derives helicity $K = \int_V \boldsymbol{A} \cdot \boldsymbol{B}\, dV$ as the necessary conserved quantity. Although, the details presented are vague and difficult to follow thus I prefer to discuss Paul Bellan's [2] derivation of the necessary differential equation $\nabla \times \boldsymbol{B} = \lambda \boldsymbol{B}$ using global helicity to minimize energy inside the system!

5.1 Minimizing Magnetic Energy under Helicity Constraint

We wish to describe this relaxed state with minimum energy consistent with (i) boundary condition $\boldsymbol{B}\cdot\hat{\boldsymbol{n}} = 0$ everywhere on S and (ii) the initial global helicity. Consider a plasma with low β, implying the plasma forces are predominantly magnetic, enclosed in a simply-connected, perfectly conducting surface S surrounding volume V. A perfectly conducting boundary implies a flux conserving system, that is, $\boldsymbol{B}\cdot\hat{\boldsymbol{n}} = 0$ everywhere on S. Suppose the plasma is initially not in equilibrium, possibly undergoing magnetic reconnections described in an earlier section. By assumption all the magnetic energy in this isolated configuration is free energy, meaning energy that can be extracted from the system as work. When the plasma configuration expels all it's free energy then it is at the point of minimum energy, this is the Taylor State, and the energy releasing transition is Taylor Relaxation. As discussed in a previous section, magnetic reconnections conserve helicity but not necessarily magnetic energy.

Since $\boldsymbol{B}\cdot\hat{\boldsymbol{n}} = 0$ this means there is no flux through every infinitesimal area of S, thus, the flux $d\psi = \oint_C \boldsymbol{A}\cdot d\boldsymbol{x} = 0$ where C is a contour around the perimeter of an infinitesimal surface $d\boldsymbol{s}$. Since $d\psi = 0$ we conclude the component of $\boldsymbol{A}$ tangential to S vanishes, or at most is the gradient of a scalar function. But, since S is a perfect conductor, the tangential component of magnetic field vanishes on S and so there cannot be any change in the tangential component of vector potential thus $\delta\boldsymbol{A}_\parallel = 0$ where $\delta \equiv \frac{\partial}{\partial t}$ the time derivative.

Now we simply need to reduce the total magnetic energy $W = \int_V \frac{B^2}{2\mu_0} dV$ subject to the helicity constraint $K = \int_V \boldsymbol{A}\cdot\boldsymbol{B} dV$ and boundary condition $\delta\boldsymbol{A} = 0$ on S. This reduces to the calculus of variations problem of minimizing W setting the variation $\delta W = 0$. We can factor in the helicity constraint by adding a Lagrange multiplier of helicity. Hence we want to minimize

$$\delta W - \lambda\delta K = \int_V \boldsymbol{B}\cdot\delta\boldsymbol{B} - \lambda\int_V (\boldsymbol{A}\cdot\delta\boldsymbol{B} + \boldsymbol{B}\cdot\delta\boldsymbol{A})dV = 0.$$

Using $\delta\boldsymbol{B} = \nabla\times\delta\boldsymbol{A}$ we have

$$\int_V \boldsymbol{B}\cdot(\nabla\times\delta\boldsymbol{A})dV - \lambda\int_V (\boldsymbol{A}\cdot(\nabla\times\delta\boldsymbol{A}) + \boldsymbol{B}\cdot\delta\boldsymbol{A}) = 0.$$

Using the memorable vector identity $\nabla\cdot(\boldsymbol{F}\times\boldsymbol{G}) = \boldsymbol{G}\cdot(\nabla\times\boldsymbol{F}) - \boldsymbol{F}\cdot(\nabla\times\boldsymbol{G})$ we have

$$\int_S (\delta\boldsymbol{A}\times\boldsymbol{B})\cdot d\boldsymbol{s} + \int_V \delta\boldsymbol{A}\cdot(\nabla\times\boldsymbol{B})dV - \lambda\int_S (\delta\boldsymbol{A}\times\boldsymbol{A})\cdot d\boldsymbol{s} - 2\lambda\int_V \boldsymbol{B}\cdot\delta\boldsymbol{A} dV = 0.$$

Since $\delta\boldsymbol{A}_\parallel = 0$ the surface integrals vanish and so we have

$$\int_V \delta\boldsymbol{A}\cdot(\nabla\times\boldsymbol{B} - \lambda\boldsymbol{B})dV = 0$$

and since $\delta\boldsymbol{A}$ is an arbitrary potential inside V the integrand vanishes and we derive the constraint for $\boldsymbol{B}$ inside of V

$$\nabla\times\boldsymbol{B} = \lambda\boldsymbol{B}.$$

Magnetic fields satisfying this equation are called Taylor states and sometimes Woltjer-Taylor states [11][13]. Using Amperes law in differential form, $\nabla\times\boldsymbol{B} = \mu_0\boldsymbol{J}$, we have that

$$\mu_0\boldsymbol{J} = \lambda\boldsymbol{B},$$

which implies that $\boldsymbol{B} = \frac{\mu_0}{\lambda}\boldsymbol{J}$. Now, since we assumed $\beta \approx 0$ we can disregard the ∇P term in the Force Balance equations which implies

$$\rho\frac{d\boldsymbol{v}}{dt} = \boldsymbol{J} \times \boldsymbol{B} - \nabla P \approx \boldsymbol{J} \times \boldsymbol{B} = \boldsymbol{J} \times \left(\frac{\mu_0}{\lambda}\boldsymbol{J}\right) = 0$$

which shows that the plasma configuration is force-free and implies the Lorentz force $\boldsymbol{F} = q(\boldsymbol{E} + \boldsymbol{v} \times \boldsymbol{B}) = 0$.

5.2 Interpreting the Eigenvalue λ

Moreover, the eigenvalue can be computed in terms of conceptually enlightening quantities [2][3]. We can rewrite the magnetic energy defined above as

$$\begin{aligned} W &= \int_V \frac{B^2}{2\mu_0}\,dV = \frac{1}{2\mu_0}\int_V \boldsymbol{B} \cdot \boldsymbol{B}\,dV = \frac{1}{2\mu_0}\int_V \boldsymbol{B} \cdot (\nabla \times \boldsymbol{A})\,dV \\ &= \frac{1}{2\mu_0}\int_V [\nabla \cdot (\boldsymbol{A} \times \boldsymbol{B}) + \boldsymbol{A} \cdot (\nabla \times \boldsymbol{B})]\,dV \\ &= \frac{1}{2\mu_0}\int_V [\nabla \cdot (\boldsymbol{A} \times \boldsymbol{B}) + \lambda\boldsymbol{A} \cdot \boldsymbol{B}]\,dV \end{aligned}$$

using the vector identity $\boldsymbol{B} \cdot (\nabla \times \boldsymbol{A}) = \nabla \cdot (\boldsymbol{A} \times \boldsymbol{B}) + \boldsymbol{A} \cdot (\nabla \times \boldsymbol{B})$. Now integrating, we have

$$\int_V \nabla \times \boldsymbol{B}\,dV = \int_V \lambda\boldsymbol{B}\,dV$$

$$\boldsymbol{B} = \lambda\boldsymbol{A} + \nabla f$$

for some scalar function f. Now we have the right and left term as

$$\begin{aligned} \int_V \nabla \cdot (\boldsymbol{A} \times \boldsymbol{B})\,dV &= \int_V \nabla \cdot (\boldsymbol{A} \times (\lambda\boldsymbol{A} + \nabla f))dV = 0 + \int_V \nabla \cdot (\boldsymbol{A} \times \nabla f)\,dV \\ &= \int_V \nabla \cdot [f(\nabla \times \boldsymbol{A}) - \nabla \times (f\boldsymbol{A})]\,dV \\ &= \int_V \nabla \cdot (f\boldsymbol{B})\,dV - 0 \\ &= \int_S f\boldsymbol{B} \cdot d\boldsymbol{S} = 0, \end{aligned}$$

using the vector identity $\nabla \times (f\boldsymbol{A}) = f\nabla \times \boldsymbol{A} + \nabla f \times \boldsymbol{A}$, the identity $\nabla \cdot (\nabla \times \boldsymbol{A}) = 0$, applying Stokes theorem, and the assumption $\boldsymbol{B} \cdot d\boldsymbol{S} = 0$ on S for an isolated configuration. Thus we have

$$\begin{aligned} W &= \frac{1}{2\mu_0}\int_V \lambda\boldsymbol{A} \cdot \boldsymbol{B}dV \\ \lambda &= 2\mu_0\frac{W}{\int_V \boldsymbol{A} \cdot \boldsymbol{B}dV} = 2\mu_0\frac{\int_V B^2 dV}{\int_V \boldsymbol{A} \cdot \boldsymbol{B}dV} = 2\mu_0\frac{W}{K}. \end{aligned}$$

Thus λ can be conceptually thought of as $\frac{energy}{helicity}$ of the isolated configuration. It is also the case that λ, which is inferred from the initial values of the helicity invariant, determines the exact force-free configuration of the plasma [11].

6 Spheromaks

In the case of the spheromak, taking the curl of $\nabla \times \boldsymbol{B} = \lambda \boldsymbol{B}$ we have the equation $\nabla^2 \boldsymbol{B} + \lambda^2 \boldsymbol{B} = 0$, with $\lambda = 0$ on the boundary [2][11]. Taylor [12] simply lists the eigenfunction solutions to the force free equilibrium for both spherical and cylindrical coordinates.

6.1 Cylindrical Container

From Bellan's discussion [2] we see derivation in cylindrical coordinates is much simpler than that in spherical coordinates. Reproducing the argument below, suppose S is a cylinder described by cylindrical coordinates (r, ϕ, z) and make the approximation assumption that $\boldsymbol{B} \approx \exp(im\phi + ikz)$ for $m, k \in \mathbb{N}$. The z component can be written as the solution of

$$\frac{\partial^2 B_z}{\partial r^2} + \frac{1}{r}\frac{\partial B_z}{\partial r} + \left(\lambda^2 - k^2 - \frac{m^2}{r^2}\right) B_z = 0,$$

with the solution

$$B_z = B_0 J_m(\gamma r) e^{im\phi + ikz}$$

with $\gamma = \sqrt{\lambda^2 - k^2}$ and where J_m is the Bessel function $J_\alpha(x) = \sum_{m=0}^{\infty} \frac{(-1)^m}{m!\Gamma(m+\alpha+1)} (\frac{x}{2})^{2m+\alpha}$. If we split both $\boldsymbol{B}$ and ∇ operator into parallel and perpendicular components to z, the eigen-force equations becomes

$$(\nabla_\perp + ik\hat{\boldsymbol{z}}) \times (\boldsymbol{B}_\perp + B_z \hat{\boldsymbol{z}}) = \lambda(\boldsymbol{B}_\perp + B_z \hat{\boldsymbol{z}}),$$

with perpendicular component

$$\lambda \boldsymbol{B}_\perp - ik\hat{\boldsymbol{z}} \times \boldsymbol{B}_\perp = \nabla_\perp B_z \times \hat{\boldsymbol{z}}$$

and taking the cross product of this equation with z gives us

$$ik\boldsymbol{B}_\perp + \lambda \hat{\boldsymbol{z}} \times \boldsymbol{B}_\perp = \nabla_\perp B_z.$$

Thus we have a system of linear equations for variables $\boldsymbol{B}_\perp$ and $\hat{\boldsymbol{z}} \times \boldsymbol{B}_\perp$ and the solving for $\boldsymbol{B}_\perp$ we find

$$\boldsymbol{B}_\perp = \frac{\lambda \nabla_\perp \times \hat{\boldsymbol{z}} + ik\nabla_\perp B_z}{\lambda^2 - k^2}.$$

Finally substituting the equation for B_z and taking the real component we have

$$\begin{aligned}
B_r(r, \phi, z) &= \operatorname{Re}\left[\frac{iB_0}{\gamma^2}\left(\frac{m\lambda}{r} J_m(\gamma r) + k\gamma J_m'(\gamma r)\right)\right] e^{im\phi + ikz} \\
&= -\frac{B_0}{\gamma}\left(\frac{m\lambda}{\gamma r} J_m(\gamma r) + kJ_m'(\gamma r)\right) \sin(im\phi + kz) \\
B_\phi(r, \phi, z) &= \operatorname{Re}\left[\frac{B_0}{\gamma^2}\left(\frac{mk}{r} J_m(\gamma r) + \lambda\gamma J_m'(\gamma r)\right)\right] e^{im\phi + ikz} \\
&= -\frac{B_0}{\gamma}\left(\frac{mk}{\gamma r} J_m(\gamma r) + \lambda J_m'(\gamma r)\right) \cos(im\phi + kz) \\
B_z(r, \phi, z) &= B_0 J_m(\gamma r) \cos(m\phi + kz).
\end{aligned}$$

called the Chandrasekhar-Kendall equations. The lowest order solution with $m = k = 0$ giving the Lundquist solution gives us

$$B_r(r, \phi, z) = 0$$
$$B_\phi(r, \phi, z) = B_0 J_1(\lambda r)$$
$$B_z(r, \phi, z) = B_0 J_0(\lambda r)$$

all which are independent of z and ϕ and claimed to be quite accurate experimentally in long axisymmetric cylinders with $\lambda >> k$.

Taylor's discussion states different formulas [12]. In a cylinder of height h and radius a, for $\frac{h}{a} \lesssim 1.67$, a critical value, the lowest eigenvalue is

$$\lambda = \sqrt{\left(\frac{3.83}{a}\right)^2 + \left(\frac{\pi}{h}\right)^2}$$

and corresponding eigenfunctions are

$$B_r = -B_0 k J_1(lr)\cos(kz)$$
$$B_\phi = B_0 \lambda J_1(lr)\sin(kz)$$
$$B_z = B_0 k J_0(lr)\sin(kz),$$

where $kh = \pi$ and $la = 3.83$.

6.2 Spherical Container

We find that in spherical coordinates of radius a the solution eigenfunctions are a great deal more complicated, in these coordinates the solutions take the form of products of spherical Bessel functions and associated Legendre functions

$$\chi_m^n = j_m(\lambda r) P_m^n(\cos\theta) e^{in\phi}$$

and through a complicated series of omitted calculations we have

$$B_r = 2B_0 \frac{a}{r} j_1(\lambda r)\cos\theta$$
$$B_\theta = -B_0 \frac{a}{r}\frac{\partial}{\partial r}[r j_1(\lambda r)]\sin\theta$$
$$B_\varphi = \lambda a B_0 j_1(\lambda r)\sin\theta$$

where $j_1(x) = \frac{J_{3/2}(x)}{\sqrt{x}}$.

6.3 Creating the Spheromak

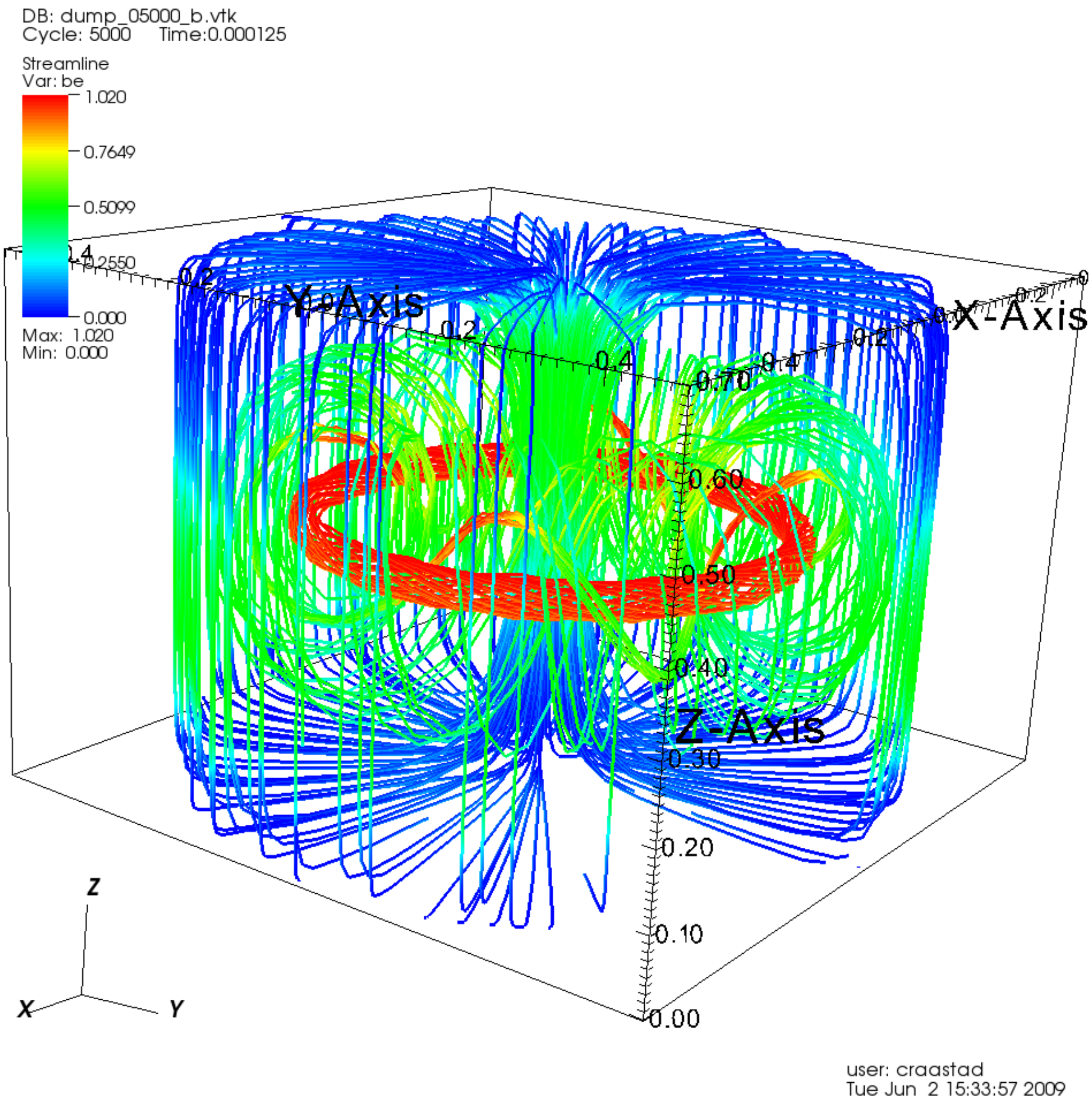

Figure 9: Magnetic Field streamline trace of a Spheromak plasma configuration created in *Visit Visualization* of data from the NIMROD simulation code courtesy of Dr. Angus McNabb.

In practical application, a Spheromak is created from initially applying a clever combination of poloidal and toroidal magnetic field, such as the plasma gun or the discharge method as mentioned in Taylor's paper [11]. After turning off certain components of field, the arbitrary collection of plasma releases it's free energy though Taylor relaxation and settles into the force free state, which in a singly connected container results in a Spheromak. The streamline in Figure 9 gives a beautiful visualization a Spheromak created in a cylindrical container governed by equations above. Typically, Spheromaks are more stable in cylindrical than spherical containers. Notice the different classes of field lines with different amounts of toroidal and poloidal field. The mostly blue lines are almost nearly completely poloidal and circulate up and down through hole of the toroidal structure. The red fieldlines are almost nearly completely toroidal and circulate around the toroidal structure. Lastly, we have field lines with about equal components of toroidal and poloidal field of varying magnitude that oscilate widely poloidal toroidally around the toroidal structure. In practical application, fusion researchers are experimenting with stability of the Spheromak as a possibility method for fusion confinement.

7 Ball Lightning/Magnetic Knots

Ball Lighting, also known as St. Elmo's Fire in folklore, is an enigmatic electromagnetic phenomenon describing a small bright "fireball" with unusual lifespan and unpredictable dynamics created in, one scenario, from lightning strikes. It's existence is somewhat controversial due to it's extreme rarity, lack of certain photographic evidence, and mostly, the difficulty to reproduce Ball Lightning experimentally in a form conforming to eyewitnesses. Two decades of work by Antonio F. Rañada applied to Ball Lightning are summarized in a paper by Rañada, Soler, and Trueba [10]. The paper discusses a reasonable explanation of Ball Lighting, that I will summarize below, by employing a topological model centered around the concept of "Magnetic Knots," an electromagnetic structure composed of helicity conserved closed and knotted electromagnetic field loops. For further reading, the mathematically sophisticated and enlightening concepts of Topological Electromagnetism and Knotted Solutions to Maxwell's equations are rigorously proposed in two of Rañada's papers [8] and [9].

Rañada introduces the idea of the topological model for Ball Lightning. Earlier work indicated that linking of plasma streamlines and magnetic lines has a stabilizing effect on the configuration, a clue to explaining the most difficult part of the Ball Lightning mystery. Assuming Ball lightning actually exists, the model proposes that

a.) Only a small part of the fireball consists of plasma of ionized air forming about 10^{-6} of the volume. This explains the overall low radiation of ball lightning and why it's luminance if equivalent to that of a household light bulb.

b.) The plasma is confined inside closed 'streamers', very narrow channels of ionized air along which electric current flows. Since air at ambient temperature does not conduct, these streamers are separated. linked in some sort of knot, like that in Figure 9.

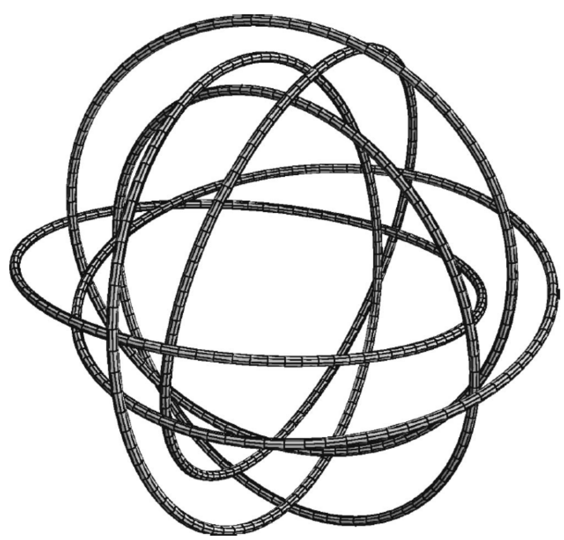

Figure 10: A complicated magnetic knot. Any two of the six lines are linked once. This also represents electromagnetic streamers along which current flows inside the fireball [10].

c.) A magnetic field with linked and knotted field lines, possibly like Figure 10, is coupled to the streamers.

Moreover, the lightning ball is not really in equilibrium, but actually in expansion (which looks like equilibrium because of the minute size of the ball). Also, the lightning ball isn't purely electromagnetic but subjected to thermodynamic considerations. Now we can summarize the stability properties as a consequence of

a.) the relaxation of the magnetic field to a force-free configuration, the same as discussed above.

b.) some solutions of Magnetic field obey the so called Alfven conditions, under which the lightning balls would remain stationary in the MHD approximation, neglecting radiation.

c.) the conservation of the Helicity integral as defined above.

Rañada then asserts the result of an experiment by Alexeff and Rader which confirms the creation of closed magnetic loops from short circuited streamers, that is, discharges about the order of 10 Megavolts. These loops are said to "contract quickly becomeing compact force-free loops that superficially resemble spheres" and "may be precursors to ball-lightning". In consequence we can safely assume under strongly stocastic conditions around the discharges (such as lightning strikes in special conditions) these closed loops can form.

Citing his own paper, [8], knotted solutions of Maxwells' equations are defined such that their force lines are closed curves and that any pair of magnetic or electric lines is a link, that is turns around each other a fixed number of times, that is product of linking numbers $n_m n_e$. For ball lightning's concern, we only consider a purely magnetic field with $\boldsymbol{E} = 0$. Suppose the magnetic knot can be represented by a scalar function $\phi(\boldsymbol{x})$ for $\boldsymbol{x} \in V$ where V is a volume where the field lines vanish outside. Consider the usual definition of helicity, $K = \int_V \boldsymbol{A} \cdot \boldsymbol{B}\, dV$. Now, with a weakly resistive plasma, in the MHD approximation, we have the following resistive Ohm's law, $\mu\boldsymbol{J} = \boldsymbol{E} + \boldsymbol{v} \times \boldsymbol{B}$ where μ is resistivity, $\boldsymbol{J}$ is current and $\boldsymbol{v}$ is fluid velocity. By assumption of V we have

$$\frac{dK}{dt} = -2\int_V \boldsymbol{E} \cdot \boldsymbol{B} dV = -2\int_V \mu\boldsymbol{J} \cdot \boldsymbol{B} dV.$$

Clearly K is conserved if $\mu\boldsymbol{J} = 0$, otherwise field lines may break and reconnect as discussed in an earlier section. Now, as discussed in one of the two of Rañada's papers referenced above, any magnetic field knot can be written as

$$\boldsymbol{B} = \frac{b}{L^2}\boldsymbol{f}\left(\frac{\boldsymbol{x}}{L}\right)$$

where L is a length scale, $\boldsymbol{f}$ a vector function, and b a normalization constant to make the dimensions make sense.

Now, when consider a force free configuration, that is, where $\nabla \times \boldsymbol{B} = \lambda\boldsymbol{B}$ Voslamber and Callebaut [10, p.21] interpreted this in two ways

a.) all the minimum energy states are force-free fields

b.) force free fields may contain huge amounts of energy.

which, under Taylor relaxation, the plasma decays to a minimum of the energy that has a force-free configuration, and this final state is stable because the magnetic force on the current vanishes and the system cannot lose energy by rearranging it's streamlines. Now under the MHD approximation goverened by the Navier Stokes equations and Maxwell equation of the magnetic field; if $\boldsymbol{v}$ is plasma velocity, p is pressure, and ρ is density, then we have the following,

$$\frac{\partial \boldsymbol{v}}{\partial t} + (\boldsymbol{v} \cdot \nabla)\boldsymbol{v} = -\frac{1}{\rho}\nabla\left(p + \frac{B^2}{2\mu_0}\right) + \frac{1}{\mu_0\rho}(\boldsymbol{B} \cdot \nabla)\boldsymbol{B},$$

$$\frac{\partial \boldsymbol{B}}{\partial t} = \nabla \times (\boldsymbol{v} \times \boldsymbol{B}) + \frac{1}{\sigma\mu_0}\nabla^2 \boldsymbol{B},$$

where $\mu_0 = 4\pi \times 10^{-7}$ Wb/A m is vacuum magnetic permeability and σ is conductivity. When $\sigma = \infty$ then

$$\boldsymbol{v} = \pm\frac{\boldsymbol{B}}{\mu_0\rho}, \quad p + \frac{B^2}{2\mu_0} = \text{const.}$$

are stationary solutions; these are called the Alfven conditions. By being a force-free magnetic field, then $\boldsymbol{B}$ and $\boldsymbol{J} = \frac{\nabla\times\boldsymbol{B}}{\mu_0}$ are parallel in the MHD approximation (as derived earlier). It follows that in a force-free magnetic field, the Alfven conditions imply that both the electrons and the ions move along the magnetic lines in opposite directions.

Now Ball Lightning formation in the topological model consists of two steps

a.) *Linking of the lines*: Near discharge of ordinary lightning, where air is ionized and streamers are formed, powerful electromagnetic forces may cause streamers to short circuit and link with one another, generating closed loops that behave like conducting linked coils. Also the corresponding magnetic field lines with the system are linked, contributing a non-zero value of helicity.

b.) *Relaxation to a force-free configuration*: A rapid Taylor relaxation process occurs almost instantaneously resulting in a force-free magnetic knot coupled to the plasma inside the ion streamers. The plasma is hot enough, in which resistivity is low enough, such that the helicity integral is conserved. Now because of the force free condition and Alfven condition, the magnetic field is parallel to the current such that ions and electrons move along streamers in opposite directions. It follows that the current streamers and magnetic field lines have the same linking numbers.

Since the feasibility of the creation of the fireball has been established, it is necessary to discuss it's evolution and death. Once the fireball has formed as described above, streamers of a fireball are within a certain sized sphere, but magnetic field lines extend further off, vanishing at infinity. But we cannot have equilibrium in this open system, thus an expansion occurs since magnetic pressure cannot be compensated for. This energy balance forces the energy that ball loses by expanding to be equivalent to the energy the fireball radiates away as brightness. The total energy of the system can be expressed as

$$E = \frac{B^2 g_n}{\mu_0 L}$$

where L is the radius of the smallest sphere containing all the streamers, and g_n is a constant depending on $\boldsymbol{B}(\boldsymbol{x})$ and the linking number n of the magnetic knot. Now an adiabatic expansion occurs implying that $L \propto \frac{1}{\sqrt{T}}$, explaining the slowness of the expansion. Also, the streamers cool in this expansion, thus decreasing continuity, producing a deviation from helicity conservation. When the conductive decreases past a critical point, the fireball ends it's life as plasma containment ceases.

References

[1] Colin C. Adams. *The Knot Book*. W. H. Freeman and Company, 1994.

[2] Paul M. Bellan. *Spheromaks*. Imperial College Press, 2000.

[3] Paul M. Bellan. *Fundamentals of Plasma Physics*. Cambridge University Press, 2006.

[4] M. A. Berger and G. B. Field. The topological properties of magnetic helicity. *Journal of Fluid Mechanics*, 147:133–148, October 1984.

[5] Jeffrey P Freidberg. *Ideal magnetohydrodynamics.* Plenum Press, 1987.

[6] H. K. Moffatt and Renzo L. Ricca. Helicity and the calugareanu invariant. *Proceedings of the Royal Society London A*, 439:411–429, November 1992.

[7] Hans Pfister and Walter Gekelman. Demonstration of helicity conservation during magnetic reconnection using christmas ribbons. *American Journal of Physics*, 59(6):497–501, June 1991.

[8] Antonio F Ranada. Knotted solutions of the maxwell equations in vacuum. *Journal of Physics A: Mathematical and General*, 23:L815–L820, April 1990.

[9] Antonio F Ranada. Topological electromagnetism. *Journal of Physics A: Mathematical and General*, 25:1621–1641, July 1992.

[10] Antonio F. Ranada. Ball lightning as a force-free magnetic knot. *Physical Review*, 62(5):7181–7190, November 2000.

[11] J. B. Taylor. Relaxation of toroidal plasma and generation of reverse magnetic fields. *Physical Review Letters*, 33(19):1139–1141, November 1974.

[12] J. B. Taylor. Relaxation and magnetic reconnection in plasmas. *Reviews of Modern Physics*, 58(3):741–763, July 1986.

[13] L. Woltjer. A theorem on force-free magnetic fields. *Proceedings of the National Academy of Sciences*, 44(6):489–491, May 1958.